Chemistry Europe
European Chemical Societies Publishing

WILEY VCH

Excellence in Chemistry Research

Announcing our new flagship journal

- Gold Open Access
- Publishing charges waived
- Preprints welcome
- Edited by active scientists

Meet the Editors of *ChemistryEurope*

Luisa De Cola
Università degli Studi di Milano Statale, Italy

Ive Hermans
University of Wisconsin-Madison, USA

Ken Tanaka
Tokyo Institute of Technology, Japan

Chemistry–A European Journal
Research Article
doi.org/10.1002/chem.202300497
Chemistry Europe
European Chemical Societies Publishing
www.chemeurj.org

Phase-Dependent Long Persistent Phosphorescence in Coumarin-Phosphine-Based Coinage Metal Complexes

Vanitha R. Naina,[a] Akhil K. Singh,[a] Pascal Rauthe,[b] Sergei Lebedkin,[c] Michael T. Gamer,[a] Manfred M. Kappes,[b, c] Andreas-Neil Unterreiner,[b] and Peter W. Roesky*[a]

Abstract: A coumarin functionalized aminodiphosphine has been introduced as a bidentate ligand in coinage metal chemistry. Mono-, di-, and trimetallic copper and silver complexes were synthesized with this ligand. The hybrid character of the ligand led to compounds with rich luminescence properties. These include coumarin-based blue fluorescence, observed as a sole emission in solution at room temperature, and green phosphorescence, which is efficient at low temperatures and dominates the spectra of the metal complexes. In the rigid environment of frozen solutions, the green phosphorescence shows an unusually long (for metal complexes) decay on the seconds timescale in high quantum yield. In addition, a red phosphorescence, which may be assigned to the triplet state localized in the phosphine-M_3Cl_2 (M=Cu, Ag), is observed for the trinuclear complexes at low temperature. Neither the second-long phosphorescence nor the red emission is observed for the coumarin ligand, thus they must be a result of the coordination to coinage metal clusters. The excited states in these compounds were also investigated by femtosecond transient absorption spectroscopy and quantum chemical calculations.

Introduction

Long persistent luminescence (also referred to as after-glow) is usually associated with inorganic phosphors.[1–4] Organic or organometallic molecules showing second-long phosphorescence remain relatively rare, although they have gained an increased research interest in the last years and their number has been steadily growing.[5–7] Most organometallic compounds, which show long phosphorescence, are metal-organic frameworks (MOF).[8,9] Many of these materials are based on zinc complexes.[10,11] Moreover, long persistent phosphorescence is usually observed in the solid-state, where intermolecular interactions such as π-stacking might play a crucial role. In contrast, long phosphorescence is not observed in frozen solutions of organometallic compounds.

In contrast to zinc compounds, the phosphorescence lifetimes of numerous known coinage metal complexes are typically limited to a microseconds to milliseconds range, both at low and ambient temperatures.[12–20] In general, coinage metal phosphine complexes have attracted significant attention due to the ease of coordination of phosphine donors with metal centers, as well as to their potential to support metallophilic interactions, which often lead to supramolecular architectures with fascinating optical properties.[21–23] In this context, diphosphine ligands have been elaborated as especially useful because of their ability to act as chelates, monodentate or bridging ligands, allowing for the spatial proximity of the metal centers and thereby resulting in stabilization of homo- and hetero-nuclear metal complexes.[24,25]

It has been well established that the introduction of additional, photophysically "active" groups into a ligand backbone can significantly alter optical properties of the related metal complexes, in particular their photoluminescence (PL). A related approach has recently been proposed for a design of organic molecules with persistent phosphorescence, by covalently linking two units, one of which providing for efficient intersystem crossing (ISC) and the second one possessing the otherwise inefficiently formed but long-lived emitting triplet state.[26] In this work, our attention was drawn to coumarin dyes as such groups, to modify PL properties of diphosphine-based coinage metal complexes. These dyes consist of a fused benzene and α-pyrone ring and belong to the family of compounds with a 2*H*-1-benzopyran-2-one core structure. Typically, coumarins are associated with bright fluorescence in solution, and consequently several coumarin derivatives serve as highly efficient, standard laser dyes for the blue–green

[a] V. R. Naina, Dr. A. K. Singh, Dr. M. T. Gamer, Prof. Dr. P. W. Roesky
Institute of Inorganic Chemistry
Karlsruhe Institute of Technology
Engesserstraße 15, 76131 Karlsruhe (Germany)
E-mail: roesky@kit.edu
Homepage: http://www.aoc.kit.edu/AK%20Roesky.php
[b] P. Rauthe, Prof. Dr. M. M. Kappes, Prof. Dr. A.-N. Unterreiner
Institute of Physical Chemistry
Karlsruhe Institute of Technology
Fritz-Haber-Weg 2, 76131 Karlsruhe (Germany)
[c] Dr. S. Lebedkin, Prof. Dr. M. M. Kappes
Institute of Nanotechnology
Karlsruhe Institute of Technology
Hermann-von-Helmholtz-Platz 1
76344 Eggenstein-Leopoldshafen (Germany)

Supporting information for this article is available on the WWW under https://doi.org/10.1002/chem.202300497

emission spectral range. However, by changing the substituents in the coumarin structure, the HOMO–LUMO energy gap as well as the character of excited states [e.g., (n,π*) vs. (π,π*)] can be modulated, strongly affecting optical and PL properties.[27–28] Furthermore, several coumarin-based platinum, ruthenium and iridium phosphorescent complexes have been reported, demonstrating a PL lifetime in the range of microseconds.[29–34]

To the best of our knowledge, only a handful of studies have dealt with the synthesis of coinage metal complexes containing coumarin in the ligand backbone,[35–38] and only in few works, the photophysical properties of the respective complexes have been explored.[39,40] Herein, we describe the synthetic approach to a novel coumarin-functionalized diphosphine ligand. The latter has been applied to obtain mono-, di-, and trinuclear copper and silver complexes. Unusually complicated PL behavior was found for these compounds, including multiband emission spectra and strong temperature and phase (solid vs. solution) dependences. We also show that the nuclearity of the metal complexes/clusters has a significant influence on the PL. Perhaps the most remarkable PL feature is a bright green phosphorescence, decaying visually for seconds after shutting down the UV excitation light, which was observed for frozen solutions of the ligand and metal complexes in dichloromethane or acetonitrile. To the best of our knowledge, we report the first example of persistent phosphorescence in this class of compounds.

Results and Discussion

Synthesis and characterization

As a coumarin functionalized ligand we chose an aminodiphosphine scaffold, in which the coumarin dye can be attached in a one-step synthesis. It is well established that the aminodiphosphine scaffold is a versatile ligand in coordination chemistry.[25] The desired ligand **L**^{1} was obtained in a one pot reaction by reacting 7-amino-4-methylcoumarin with an excess of triethylamine and 2.5 equivalents of chlorodiphenylphosphine in tetrahydrofuran (THF) and was isolated in 67% yield (Scheme 1).

The molecular structure of **L**^{1} in the solid-state (Figure 1) reveals a P–N–P angle of 114.20(7)° and P–N bond distances of 1.732(13) Å (P1–N) and 1.724(11) Å (P2–N), which are in accordance with related aminodiphosphines reported in the literature.[41] The successful deprotonation of 7-amino-4-methylcoumarin was confirmed unambiguously by the ^{1}H NMR spectrum. Additionally, the appearance of aromatic signals of diphenylphosphine in ^{1}H NMR (δ 7.40–7.23) and a singlet signal in the ^{31}P{^{1}H} NMR spectrum (δ 68.7 ppm) are observed.

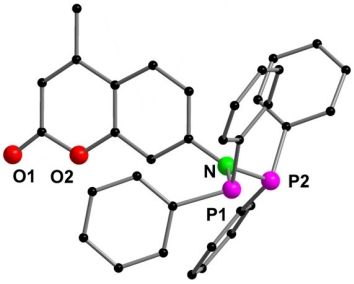

Figure 1. Molecular structure of aminodiphosphine **L**^{1} in the solid state. Hydrogen atoms and non-coordinating solvent molecules are omitted for clarity. Structural parameters are given in Figure S32 in the Supporting Information.

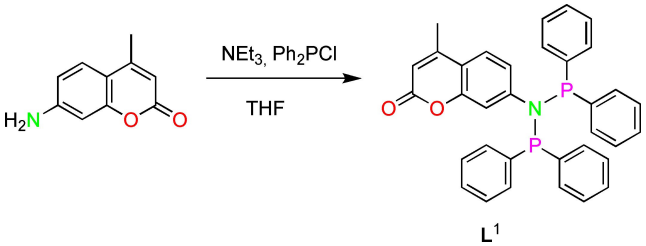

L^1

Scheme 1. Synthesis of ligand **L**^{1} starting from 7-amino-4-methylcoumarin.

Aminodiphosphine (PNP) ligands are well-known for their chelating and bridging coordination with metals. Compound **L**^{1} was further introduced as a ligand for synthesizing suitable copper and silver complexes (Schemes 2 and 3, below). The reaction between **L**^{1} and $Cu(CH_3CN)_4PF_6$ was carried out in 2:1 molar ratio and yielded the Cu complex **1** with two chelating **L**^{1} ligands in 85% yield. Suitable crystals for X-ray diffraction analysis were grown by slow diffusion of diethyl ether into a concentrated CH_2Cl_2 solution of **1**.

The molecular structure of **1** is displayed in Figure 2. The Cu^I cation is coordinated with four phosphorus atoms of the two ligand moieties in a distorted tetrahedral geometry with P–Cu–P angles ranging from 74.20(2)° to 131.79(2)°. The ^{31}P{^{1}H} NMR shows a singlet at δ 89.6 ppm which is downfield-shifted when compared to the free ligand and another septet at δ 144.3 ppm corresponding to the PF_6 counter anion. The observed phosphine signal is similar to other copper complexes.[42]

A simple modification of the reaction conditions leads to formation of dinuclear and trinuclear copper complexes (Scheme 2). The dinuclear compound **2** was synthesized by reacting equimolar amount of the ligand **L**^{1} with $Cu(CH_3CN)_4BF_4$. Crystals of **2** were obtained by slow evaporation of acetone solution of **2** in a sealed ampoule.

The molecular structure of **2** in the solid state consists of two copper(I) cations coordinated to the two phosphines of the ligand in a bridging mode (Figure 2). In addition, one acetone molecule is coordinated to each Cu^I cation and an additional acetone molecule is bridging between both the Cu centers which might be playing a crucial role in stabilization of the molecular structure. The Cu1···Cu2 separation between two Cu^I cations is 2.842(10) Å which is close to the upper limit of cuprophilic interactions.[43–44] Therefore, the copper ion adopts a distorted tetrahedral geometry with weak, if any, metallophilic interactions. PNP bridging ligands along with the copper cations form an eight-membered ring which adopts a twist-

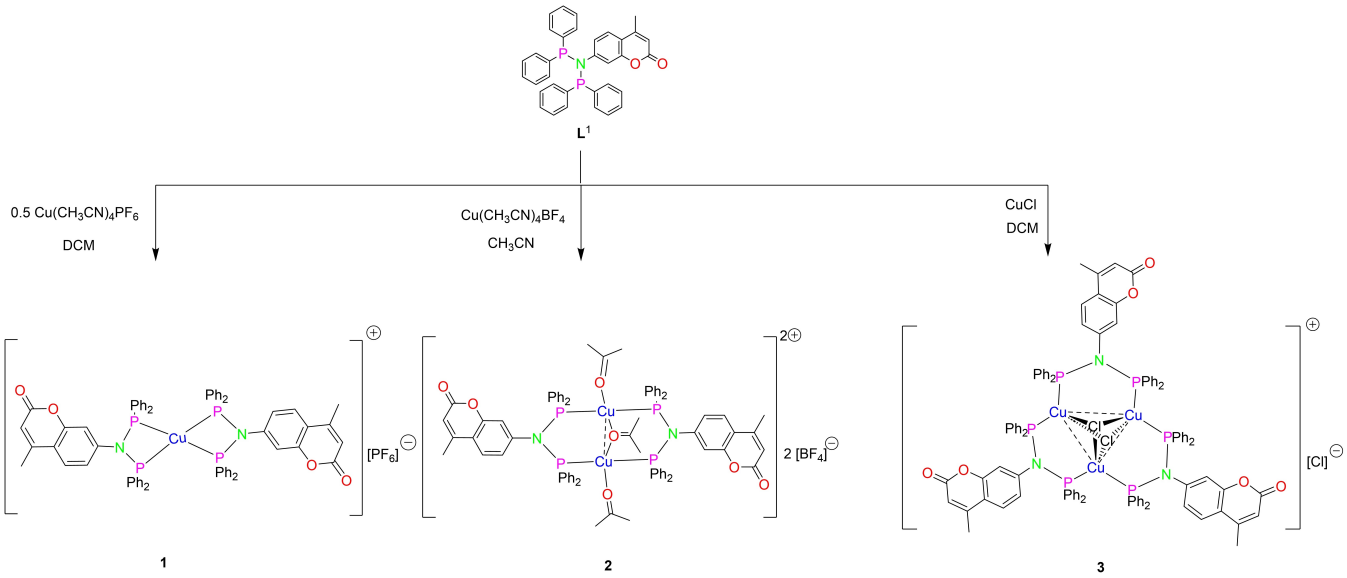

Scheme 2. Synthesis of mono- (**1**), di- (**2**), and trinuclear (**3**) copper complexes starting from **L**[1].

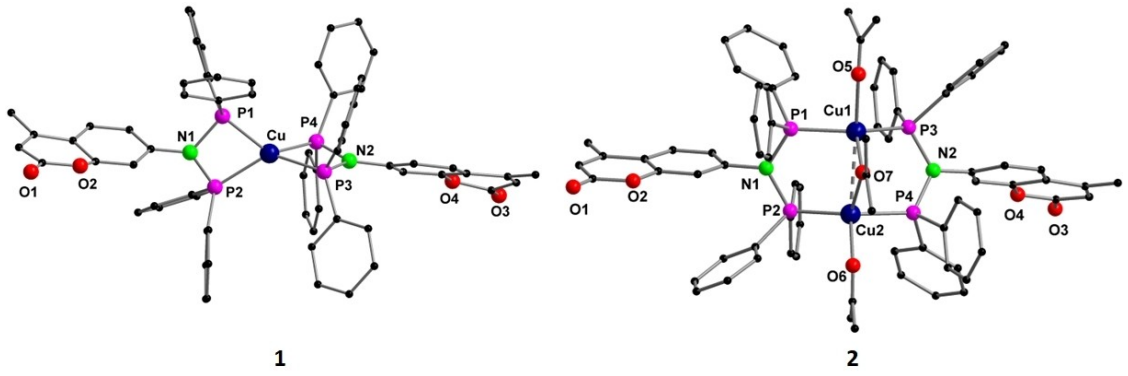

Figure 2. Molecular structure of complexes **1** and **2** in the solid state. Hydrogen atoms and non-coordinating solvent molecules are omitted for clarity. Structural parameters are given in Figures S33 and S34.

boat conformation in accordance with reports in the literature.[45]

Reacting the ligand **L**[1] with CuCl in 1:1 ratio resulted in the formation of trinuclear Cu complex **3** (Scheme 2). Unfortunately, only low quality crystals not perfectly suitable for XRD analysis were obtained. However, it was possible to extract the connectivity from the difference Fourier map. Compound **3** consists of a Cu_3Cl_2 core, with the three Cu^I cations forming an almost equilateral triangle, likely to be stabilized by metallophilic interaction as reported in the literature (Figure S35).[46] Three copper cations lie on a plane with two capping μ^3-Cl ligands lying above and below the plane and are also coordinated to the phosphines of the ligands in a bridging mode. The phosphine resonance in the $^{31}P\{^1H\}$ NMR spectrum appears at δ 59.8 ppm which is upfield shifted in comparison with the free ligand (δ 68.6 ppm). HRESI-MS analysis confirmed the formation of the desired product as its molecular ion peak $[M]^+$ was detected at *m/z* 1892.1952.

Having synthesized the copper complexes, we were also interested in preparation of analogous silver complexes with different nuclearities in order to study the changes in their PL spectra. Braunstein and co-workers reported the synthesis of mono-, di-, and trinuclear silver complexes with bis(diphenylphosphino)amine ligands in 2017.[47] All the silver complexes were synthesized following a similar procedure under exclusion of light. Mononuclear Ag^I complex **4** was isolated by reacting the compound **L**[1] with $AgBF_4$ in 2:1 ratio respectively in THF overnight (Scheme 3). The desired compound precipitated out from conc. THF on addition of *n*-pentane.

Several attempts to crystallize compound **4** remained unsuccessful. However, complex formation was indicated by a distinct pattern in $^{31}P\{^1H\}$ NMR which features a doublet centered at δ 97.0 ppm in a similar range with the reported complexes.[47] The characteristic pattern also supports the presence of four equivalent phosphorus atoms coordinated to a

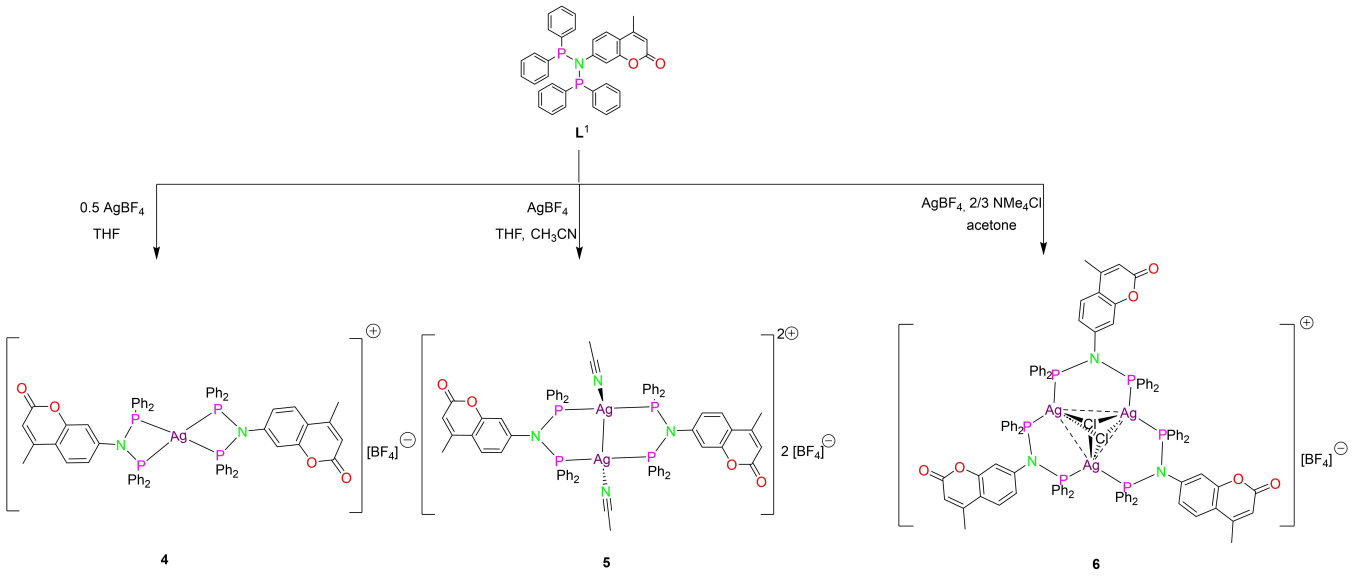

Scheme 3. Synthesis of mono- (**4**), di- (**5**), and trinuclear (**6**) silver complexes starting from $\mathbf{L}^1$.

silver cation in a tetrahedral geometry.[48] Further, HRESI-MS analysis confirmed the formation of complex **4** as its molecular ion peak $[M]^+$ was detected at *m/z* 1193.1956.

The dinuclear Ag complex **5** was isolated by reacting the ligand $\mathbf{L}^1$ with $AgBF_4$ in equimolar ratio in a mixture of THF and acetonitrile (Scheme 3). In complex **5**, the silver cations are coordinated to the diphosphines of $\mathbf{L}^1$ in a bridging mode (Figure 3). Additional coordination vacancy of Ag^I is filled by an acetonitrile molecule. The Ag···Ag separation was measured to be 2.912(6) Å which indicates the presence of argentophilic interactions (≤3.4 Å).[49] The silver cation adopts a distorted tetrahedral geometry with P1′–Ag–P2 and P1′–Ag–N2 angles to be 141.88(3)° and 106.06(9)°, respectively. The charge of the metal centers is balanced by two non-coordinating BF_4^- anions. The $^{31}P\{^1H\}$ NMR spectra of **5** revealed a pseudo triplet flanking a broad signal at δ 88.1 ppm which is similar to the complexes reported in the literature.[47]

The trinuclear Ag complex **6** was isolated on reacting the ligand $\mathbf{L}^1$ with $AgBF_4$ and NMe_4Cl in 1:1:2/3 ratio in a one-pot reaction following the literature (Scheme 3).[47] NMe_4Cl was used as a chloride source in this reaction.

Complex **6** forms a trinuclear silver structure in the solid state comprising a Ag_3Cl_2 core. It is isostructural to complex **3**, with the three Ag^I cations forming an almost equilateral triangle with Ag···Ag distances varying between 2.966(3) and 3.204(3) Å (Figure 3). The Ag_3Cl_2 is likely stabilized by argentophilic interactions (≤3.4 Å).[49] Three silver cations are coordinated to three ligands in a bridging mode and are also bonded to two

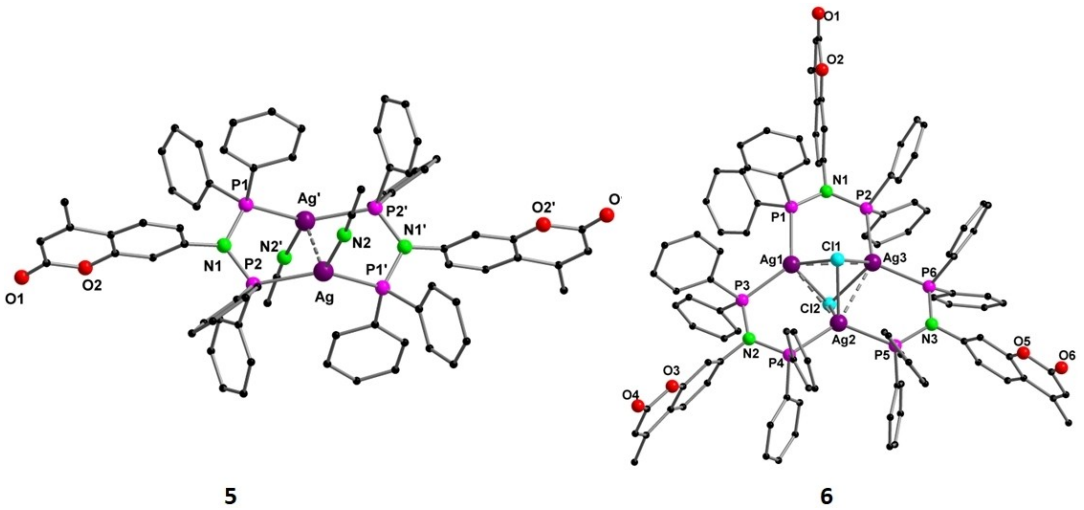

Figure 3. Molecular structure of complex **5** and **6** in the solid state. Hydrogen atoms and the non-coordinating solvent molecules were removed for clarity. Structural parameters are given in Figures S36 and S37.

capping μ_3-Cl ligands lying above and below the plane comprising the silver ions, with Ag–Cl distances between 2.650(7) and 2.750(8) Å. The overall positive charge of the metal cluster is balanced by a non-coordinated BF_4 anion.

Complexation is accompanied by the appearance of a distinct pattern in $^{31}P\{^1H\}$ NMR spectra with two broad pseudo quadruplets centered at δ 77.8 and 74.9 ppm. These characteristic patterns arise from overlapping of the different contributions of all possible isotopomers of silver as reported in the literature.[47]

Photophysical properties

Figure 4 shows absorption spectra of the ligand **L**^{1} and several metal complexes with different nuclearities, dissolved in dichloromethane (DCM) and measured at ambient temperature. The first absorption band observed for all these compounds at 320–340 nm is significantly contributed by the coumarin groups, as indicated by the absorption spectrum of 7-amino-4-methylcoumarin shown for comparison. The low energy singlet excitations are also affected by the metal complexation, since the absorption of the complexes is only roughly proportional to the number of **L**^{1} groups and also varies from one metal complex to another (Figure 4). All compounds were found to emit fast ($\tau_{PL} < 5$ ns) blue fluorescence at about 390 nm in DCM solutions (shown in Figure S38 for **L**^{1}, **3** and **4**), which can again be attributed to the coumarin groups. Supporting this assignment, the excitation spectra in Figure S38 follow absorption of the coumarin groups.

Their fluorescence is also very similar to that of 7-amino-4-methylcoumarin in DCM (Figure S39). The latter compound emits, however, with a nearly unity quantum efficiency, $\Phi_{PL} =$ 90% (i.e., similar to solutions of this laser dye in alcohols), whereas Φ_{PL} of only 0.4% was determined for its amino-diphosphine derivative, **L**^{1}. Comparably low values of Φ_{PL} were found for the mononuclear metal complexes and trinuclear silver compound in DCM (1.9, 0.63 and 1.3% for **1**, **4** and **6**, respectively). In difference, the fluorescence is enhanced in the di- and trinuclear copper complexes **2** (6.3%) and **3** (8.6%). These observations are in line with previous reports that even a small variation of substituents can strongly affect the photophysical properties of coumarins.[27–28]

No signatures of long-lived emission, that is, phosphorescence, were detected in the above solutions (thoroughly purged with argon). This changes dramatically by cooling the solutions below the freezing point (176.5 K for DCM). In such rigid environment, besides the fluorescence band at 390–400 nm, a long-lived green phosphorescence centered around 500 nm appears in the emission spectra of **L**^{1} and the metal complexes (Figure 5; see also videos in the supporting information). It is of moderate intensity and overlapped with the broadened fluorescence in case of **L**^{1}, whereas it becomes brighter and dominating in the metal complexes. This band demonstrates the same position and vibronic structure in all the spectra and can be assigned to phosphorescence of the coumarin units. Similar PL behavior was also observed for the solutions in acetonitrile (freezing point at 228.1 K). Note that only blue fluorescence and no phosphorescence were detected in frozen solutions of 7-amino-4-methylcoumarin. Femtosecond transient absorption spectroscopy revealed a fast and efficient intersystem crossing in the ligand **L**^{1} and metal complexes (see below). Accordingly, the phosphorescence is quenched in these compounds by non-radiative relaxation of their (abundant)

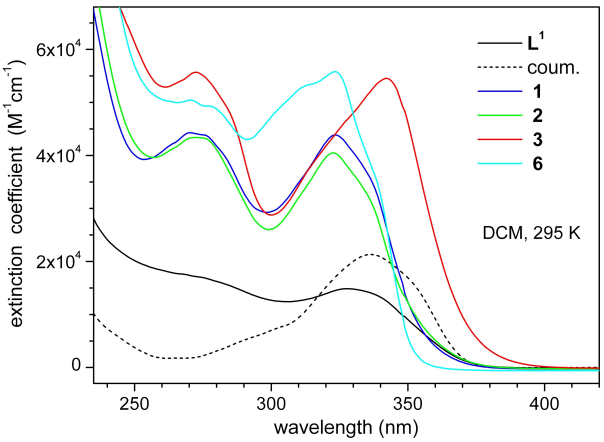

Figure 4. Absorption spectra of ligand **L**^{1} and selected copper (**1**–**3**) and silver (**6**) complexes in dichloromethane at ambient temperature. The absorption of 7-amino-4-methylcoumarin in DCM (dashed line) is also shown for comparison.

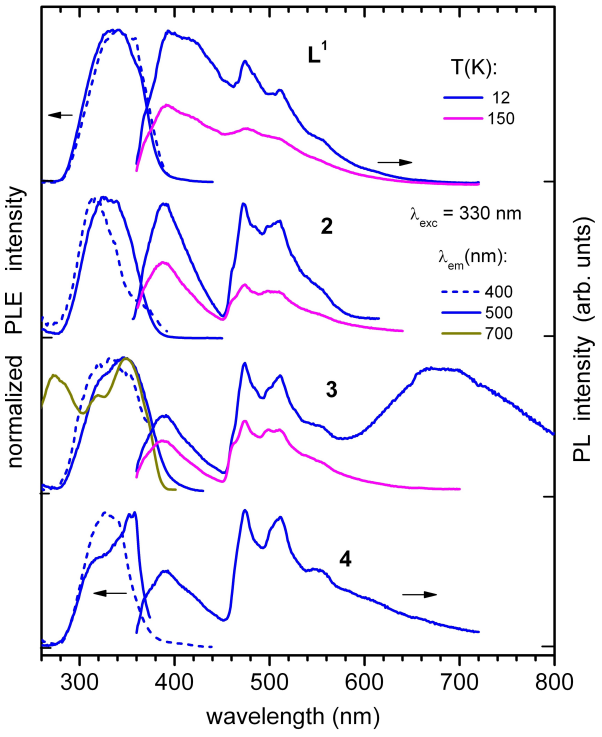

Figure 5. Photoluminescence excitation (PLE) and emission (PL) spectra of ligand **L**^{1} and copper (**2**, **3**) and silver (**4**) complexes in frozen dichloromethane at 12 and 150 K. The PLE/PL spectra were recorded/excited at the indicated wavelengths. The PLE spectrum of **3** at $\lambda_{em} = 700$ nm was measured at 12 K.

triplet state, which is apparently especially efficient in fluid solutions due to dynamic interactions with solvent molecules. The latter are hampered in solid (frozen) solutions. The intensity of both fluorescence and phosphorescence bands in frozen DCM is higher with regard to the fluorescence at ambient temperature, and further moderately increases by decreasing the temperature below 100 K (Figure 5). For instance, by comparison of the temperature-dependent spectra, we roughly estimate Φ_{PL} of the green phosphorescence of $\mathbf{L}^1$ as ~1.5% and a total emission efficiency as ~6% at 12 K. For the dissolved copper complex **3**, the fluorescence intensity does not change significantly over the whole temperature range, but the green emission amounts to Φ_{PL} ~30 and 15% at 12 and 150 K, respectively. The total PL efficiency at 12 K, including the band at 680 nm (see below), approaches 100%. The green emission is readily observed visually, for instance, in a test experiment, where a NMR tube with a solution of $\mathbf{L}^1$ or its metal complexes is inserted into liquid nitrogen (at ca. 77 K) and illuminated with an UV lamp (Figure S40). Already this simple experiment revealed an interesting property of the green phosphorescence - its second-long persistence after switching off an UV excitation source.

Figure 6 shows the respective decay traces recorded over 8 seconds for $\mathbf{L}^1$ and the trinuclear metal complexes in solid DCM at 10 and 150 K. The decay kinetics are clearly non-monoexponential over this timescale, demonstrating a distribution of characteristic decay times lifetimes in the range of 0.05–1.5 s (see videos in the Supporting Information), which likely relates

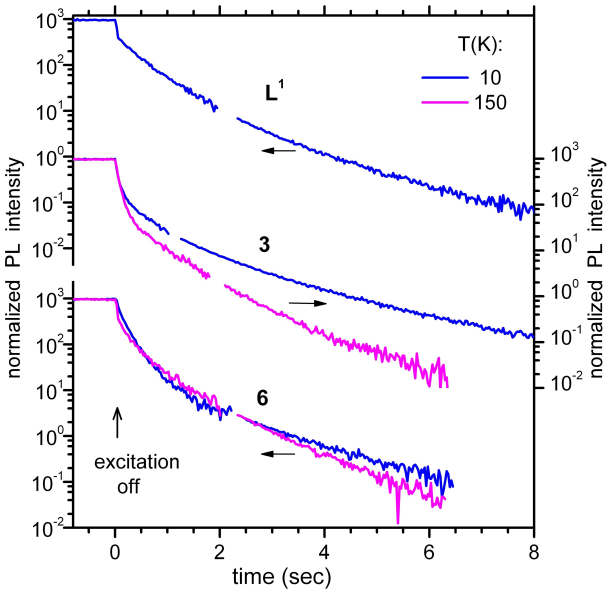

Figure 6. Decay of the long-lived green phosphorescence (cf. Figure 5) of ligand $\mathbf{L}^1$ and trinuclear copper and silver complexes **3** and **6** in frozen dichloromethane at 10 and 150 K. The decay traces were recorded at 500 nm after shutting down steady excitation at 330 nm. The initial stepwise decrease in emission intensity observed for $\mathbf{L}^1$ reflects a contribution of fast fluorescence. The gaps in the traces at about $t = 2$ s are due to removal of a neutral density filter (OD = 2, applied to extend the accessible signal range) from the emission detection channel. PL signals recorded with the filter were then upscaled to correct for the filter transmission.

to different local configurations of the emitting molecules in the frozen solution.

For instance, if approximated with triple-exponential curves, the green phosphorescence of $\mathbf{L}^1$ at 10 K decays with the following lifetimes (relative weights): 0.058 s (54%), 0.30 s (13%) and 1.01 s (33%), corresponding to an average lifetime $\langle\tau\rangle = 0.26$ s. This emission could be detected even at 10 s after switching off the UV photoexcitation. Its average lifetime decreases to 0.14 s at 150 K. Ligand $\mathbf{L}^1$ in frozen DCM at 10 K demonstrates a narrower distribution of the respective lifetimes (0.24 s (40%), 0.58 s (57%) and 1.46 s (3%)) and a slower decay with $\langle\tau\rangle = 0.48$ s. However, the persistent green phosphorescence is a minor emission in $\mathbf{L}^1$ (Figure 6), and its overall intensity is less than in the metal complexes. A similarly long-lived phosphorescence has been observed for some coumarin derivatives in frozen alcohol solutions at 77 K.[27]

The trinuclear complexes **3** and **6** in frozen DCM even demonstrate a second phosphorescence band at about 680 and 630 nm, respectively (shown for **3** in Figure 5, and video in the Supporting Information), which develops at low temperatures and becomes comparable in intensity to the green coumarin phosphorescence below ~50 K. The red emission lifetime is, however, much shorter (a few hundreds of microseconds, Figure S41). This surprising observation indicates that the excited state responsible for the red PL is essentially decoupled from the coumarin long-lived triplet. The excitation spectra of the two phosphorescence bands are also quite distinct (Figure 5). Accordingly, the red phosphorescence may be assigned to the triplet state localized in the phosphine-M_3Cl_2 (M=Cu, Ag) core structure of **3** and **6**.

It is worth comparing now the PL properties of the ligand $\mathbf{L}^1$ and metal complexes in solid (polycrystalline) state. In general, their PL spectra in the solid state reflect those observed in (frozen) DCM solutions (Figure S42). The relative intensities and temperature dependence of the PL bands are, however, different. The ligand $\mathbf{L}^1$ shows blue fluorescence centered around 400 nm and a very weak green phosphorescence band at about 500 nm, both are vibronically well-structured at low temperatures (Figure S42). In the metal complexes, the coumarin-based phosphorescence dominates the spectra, with a similar spectral position and vibronic pattern as in the frozen DCM solutions. Similar to the latter, the trinuclear metal complexes show the second, red phosphorescence band observed below ~100 K at 720 nm for **3** and at 600–650 nm for **6** (weak and overlapped with the green phosphorescence tail). A strong decrease of PL by increasing the temperature above 100 K up to 295 K appears common for the solid $\mathbf{L}^1$ and metal complexes (Figure S42). At ambient temperature, for instance, practically no PL is observed for the mononuclear Cu complex **1** and only a very weak and broad phosphorescence band for the dinuclear Cu complex **2**. Furthermore, the green phosphorescence decays now on the timescale of hundreds of microseconds-tens of milliseconds, that is, much faster than in the frozen solution at the same temperatures as illustrated for **3** and **6** in Figure S43-for comparison with Figure 6. We conclude that the PL of $\mathbf{L}^1$ and its metal complexes is strongly phase-dependent. It seems that the coumarin triplet formation is efficient in the solid state as well.

However, in this phase, the triplet relaxation appears to be strongly accelerated and dominated by non-radiative pathways at elevated temperatures. In a future study, it might be interesting to probe the photophysical behavior of these molecules deposited on a suitable substrate, to see whether their persistent green phosphorescence may be sustained in such environment, perhaps even at ambient temperature.

Transient absorption spectroscopy

The above results suggest a significant ISC, that is, triplet formation, in **L**[1] and especially in the metal complexes. We have applied transient absorption (TA) spectroscopy (for details see Supporting Information) to probe the ISC process on the timescale from tens of fs till 1.1 ns for **L**[1] and the metal complexes in DCM at ambient temperature. Figures 7 and S44–S49 present TA spectra probed in the spectral range of 350–750 nm for **3** and **L**[1] and other metal complexes at increasing delay times after fs-pulsed excitation into the first absorption band at 326 nm.

The trinuclear copper complex **3** shows TA bands, forming within 5 ps at around 400 nm and over 500–700 nm, as well as the strongest remaining absorption after 1 ns delay (at ca. 460 nm), which is assigned to the triplet excited state(s). Global fitting between 395 nm and 475 nm leads to time constants $\tau_1 = 1.6$ ps and $\tau_2 = 206$ ps, where the first likely describes S_1 relaxation and the second is attributable to ISC. We cannot quantify the ISC quantum yield, but the TA magnitude suggests that ISC is a significant relaxation channel in **3**. Note also that, despite a visually bright fluorescence of the sample solution under laser excitation, the TA response is positive over the emission range (~350–450 nm, Figure S38).

This is due to a moderate fluorescence efficiency (see above) and high extinction coefficients expected for the singlet and triplet excited states. The initial photophysical processes in **3** are further illustrated with a Jablonski diagram in Figure S50 and with TA rise and decay curves at selected probe wavelengths in Figure S51. With not much difference to **3**, the mononuclear copper complex **1** shows similar S_1 relaxation and triplet formation on a longer timescale with a smaller triplet-assigned TA around 490 nm, remaining after 1 ns delay (Figure S45). Equivalent observations were also made for the other metal complexes (see the Supporting Information). In **L**[1], the relaxation of the initial TA spectra with a maximum at 415 nm evolves to a peak at 400 nm with a time constant comparable to the ISC rate in the metal complexes. Accordingly, the time-resolved absorption spectroscopy supports a substantial triplet formation both in the ligand and metal complexes. The efficiency of this process in the ligand appears, however, notably lower than in the metal compounds, in agreement with the PL results discussed above.

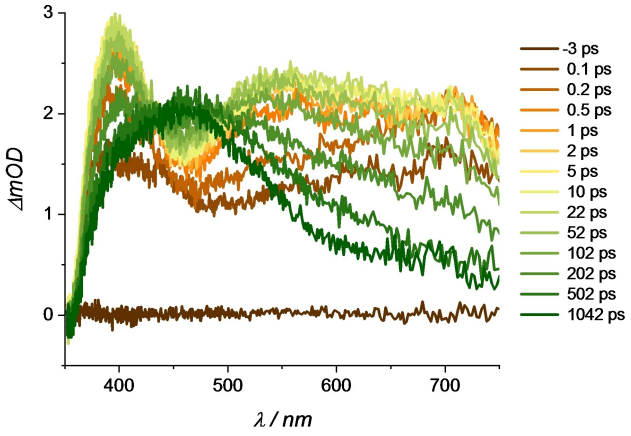

Figure 7. Transient absorption (TA) spectra of **3** in DCM at ambient temperature after fs-pulsed laser excitation at 326 nm (0.44 μJ per pulse) at increasing delay times. Initial absorption at 326 nm corresponds to OD 2.4.

Quantum chemical calculations

To get further insights into electronic properties of the ligand and metal complexes, we have carried out a series of density functional theory (DFT) and time-dependent density functional theory (TDDFT) calculations (for details see the Supporting Information). Figures S52–S58 display the frontier molecular orbitals of **L**[1] and the copper and silver complexes. In **L**[1], the HOMO (highest occupied molecular orbital) evolves over coumarin and phosphine moieties, whereas the LUMO (lowest unoccupied molecular orbital) is localized on the coumarin ring, suggesting a charge transfer character of the S_1 state (Figure S52). In all complexes, HOMOs are derived from the metal-centered orbitals with a significant contribution from the coordinating P atoms, whereas LUMOs are localized on the coumarin units. Table S4 summarizes the calculated excited state energy levels. We note that they are underestimated with regard to the experimental values (energies of the first absorption or PLE bands and phosphorescence maxima), which is rather typical for DFT calculations of states with a pronounced charge transfer character.

A general strategy to achieve bright phosphorescence is to promote the ISC and to reduce non-radiative decay of the triplet state.[50–51] A calculation of the ISC rates represents, however, a very formidable theoretical task. In a simplified approach, the requirements for an efficient ISC transition can be reduced to the following ones.[26,52–56] i) The energy of a triplet state (T_n) should lie close to that of S_1. The allowable energy difference is typically considered as ± 0.4 eV or less. ii) Singlet (S_1) and triplet (T_n) states should have a similar orbital configuration. The latter condition corresponds to a qualitative estimate of the vibronic (Frank-Condon) overlap between the transition states. This cannot estimate the ISC rates, but can distinguish between "good" and "poor" ISC-candidate T_n states (with large and small Franck-Condon overlaps, respectively). Figures 8, S59 and S60 show the corresponding energy schemes and possible ISC channels. In 7-amino-4-methylcoumarin, in agreement with experimental data, the ISC is hampered by the unfavorable orbital configuration of the triplet states energetically close to the S_1 state. The situation changes when one diphenylphosphine is attached to the coumarin: two potential

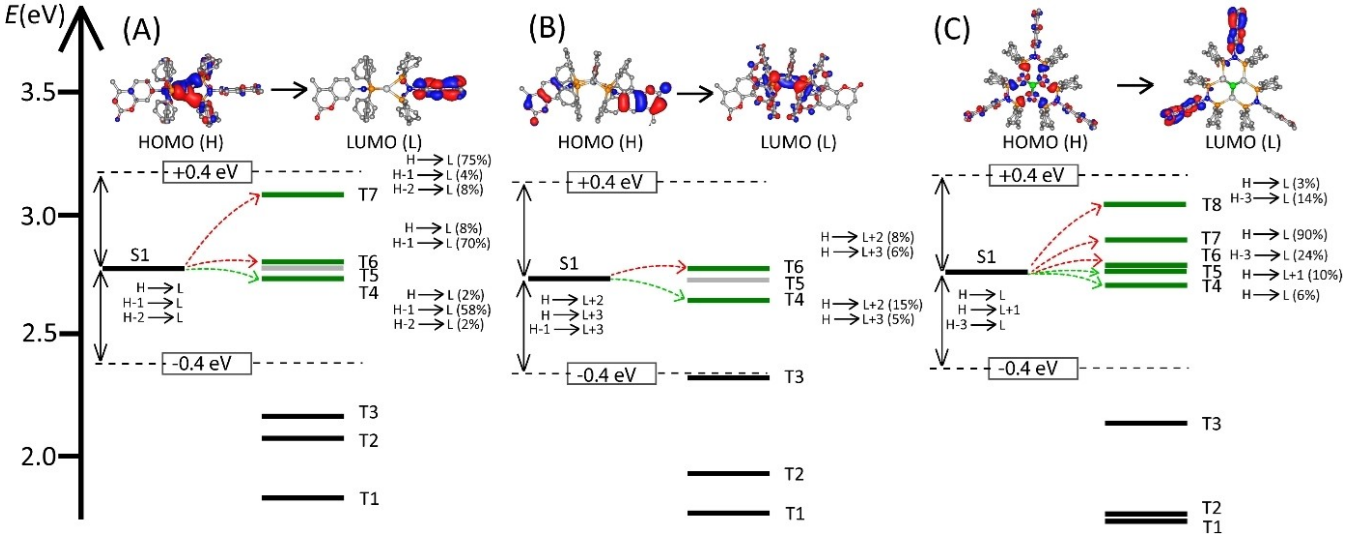

Figure 8. DFT-calculated HOMO and LUMO topologies and TD-DFT-calculated (B3LYP/LANL2DZ/6-31G** level) energy levels, main orbital configurations, and possible ISC channels for A) complex **1**, B) complex **2**, and C) complex **3**. S1: Lowest singlet excited state, T1: lowest triplet excited state, and Tn: high-level triplet excited states. Possible ISC channels occurring from the S1 state to its higher- or lower-lying triplet states (Tn) are marked with red and green dashed arrows, respectively.

ISC channels with close and favorably configured states appear from S_1 to T_5 and T_6 (Figure S59 B). In **L**[1], containing two phosphine units, there are four potential ISC channels from S_1 to $T_{4\text{-}7}$. Similar patterns were calculated for the metal complexes: they all have a few triplet states energetically close to S_1, and at least some of those states can possibly provide for efficient ISC transitions (Figures 8 and S60). Spin density distribution for triplet states T_4, T_5 and T_6 of the complex **3** were also calculated, since transition to S_1 from these states are most favorable for ISC (Figure S61). The calculation revealed that spin density mainly evolved on Cu_3Cl_2 core of the complex. This accounts for the different emission behavior of the trimetallic complexes in comparison to ligand **L**[1] and other metal complexes. However, in T_1 state, the spin density is mainly confined on the coumarin moiety in all complexes (Figure S62). Accordingly, (TD)DFT results support a significant triplet formation in **L**[1] and the metal complexes - in contrast to 7-amino-4-methylcoumarin. In addition, the rearrangement of the molecular structure upon $T_1 \rightarrow S_0$ and $S_1 \rightarrow S_0$ transitions was checked on the basis of bond lengths. In general, all structures were found to be relatively rigid, with the trimetallic systems demonstrating the most notable changes.

Conclusion

In summary, we have described a new strategy to enhance the lifetime of phosphorescence in metal complexes by introducing a coumarin dye into the backbone of an aminodiphosphine moiety. This approach not only increased the possible channel for ISC in the ligand, but also allowed us to isolate mono-, di-, and trinuclear complexes that display unusually long phosphorescence at low temperatures. TD-DFT calculations revealed a further increase in favorable ISC channels in **3** when compared to the ligand. This enhanced the long-lived green emission of **3** in solution at $\langle\tau\rangle$ values as long as 1.5 s at low temperatures ($\langle\tau\rangle$ of the ligand is 0.48 s). Apart from a prolonged lifetime, at 12 K, Φ_{PL} of **3** was estimated to reach ~100% compared to ~6% for the ligand **L**[1], thus showing the influence of the metals in this system and making it superior to other known coumarin derivatives. Furthermore, transient absorption spectroscopy results also support the idea that the triplet state is significantly pronounced in cluster compounds. Interestingly, the trinuclear complexes **3** and **6** exhibit a second phosphorescence centered at 680 and 630 nm, respectively, below ~50 K with lifetimes in the microsecond range owing to the presence of spin density on the metal core. However, at ambient temperature and in the solid state, the reported compounds phosphoresce with much shorter lifetimes than in the frozen solutions. Supported by theoretical predictions, this work could serve as a guideline to design novel ligands and to isolate long-lived phosphorescent metal complexes.

Experimental Section

The synthesis and characterization of all compounds, NMR, HRESI-MS, IR, PL spectra and transient absorption spectra, as well as X-ray crystallography and DFT calculation details are given in the Supporting Information.

Deposition Numbers 2223052 (for **L**[1]), 2223053 (for **1**), 2223054 (for **2**), 2223055 (for **5**) and 2223053 (for **6**) contain the supplementary crystallographic data for this paper. These data are provided free of charge by the joint Cambridge Crystallographic Data Centre and Fachinformationszentrum Karlsruhe Access Structures service.

Acknowledgements

V.R.N., P.R., A.N.U., and P.W.R. acknowledge GRK 2039 Molecular Architectures for Fluorescent Cell Imaging for the financial support. SL and MK acknowledge support by DFG funded Transregional Collaborative Research Centre 88 [Cooperative Effects in Homo- and Heterometallic Complexes (3MET)] (Projects C6 and C7). We also acknowledge the Karlsruhe Nano Micro Facility (KNMF) and Prof. Dr. D. Fenske for data collection on a Stoe StadiVari diffractometer with Ga-metal-jet source. Open Access funding enabled and organized by Projekt DEAL.

Conflict of Interest

The authors declare no conflict of interest.

Data Availability Statement

The data that support the findings of this study are available in the supplementary material of this article.

Keywords: aminodiphosphine · coumarin · coinage metals · persistent phosphorescence

[1] Y. Li, M. Gecevicius, J. Qiu, *Chem. Soc. Rev.* **2016**, *45*, 2090–2136.
[2] S. Wu, Y. Li, W. Ding, L. Xu, Y. Ma, L. Zhang, *Nano-Micro Lett.* **2020**, *12*.
[3] B. Mu, F. Zhao, Y. Chu, C. Li, J. Sun, Q. Zhao, S. Bai, *Eur. J. Inorg. Chem.* **2022**, e202100976.
[4] V. Liepina, D. Millers, K. Smits, *J. Lumin.* **2017**, *185*, 151–154.
[5] Y. Su, S. Z. F. Phua, Y. Li, X. Zhou, D. Jana, G. Liu, W. Q. Lim, W. K. Ong, C. Yang, Y. Zhao, *Sci. Adv. 4*, eaas9732.
[6] D. Li, J. Yang, M. Fang, B. Z. Tang, Z. Li, *Sci. Adv. 8*, eabl8392.
[7] R. Tian, S. M. Xu, Q. Xu, C. Lu, *Sci. Adv. 6*, eaaz6107.
[8] C.-Y. Zhu, Z. Wang, J.-T. Mo, Y.-N. Fan, M. Pan, *J. Mater. Chem. C* **2020**, *8*, 9916–9922.
[9] X. Yang, D. Yan, *Chem. Sci.* **2016**, *7*, 4519–4526.
[10] X.-G. Yang, Z.-M. Zhai, X.-M. Lu, J.-H. Qin, F.-F. Li, L.-F. Ma, *Inorg. Chem.* **2020**, *59*, 10395–10399.
[11] B. Zhou, G. Xiao, D. Yan, *Adv. Mater.* **2021**, *33*, 2007571.
[12] T. McCormick, W.-L. Jia, S. Wang, *Inorg. Chem.* **2006**, *45*, 147–155.
[13] T. Hofbeck, U. Monkowius, H. Yersin, *J. Am. Chem. Soc.* **2015**, *137*, 399–404.
[14] L. Bergmann, J. Friedrichs, M. Mydlak, T. Baumann, M. Nieger, S. Bräse, *Chem. Commun.* **2013**, *49*, 6501.
[15] J. M. Busch, D. S. Koshelev, A. A. Vashchenko, O. Fuhr, M. Nieger, V. V. Utochnikova, S. Bräse, *Inorg. Chem.* **2021**, *60*, 2315–2332.
[16] D. M. Zink, D. Volz, T. Baumann, M. Mydlak, H. Flügge, J. Friedrichs, M. Nieger, S. Bräse, *Chem. Mater.* **2013**, *25*, 4471–4486.
[17] V. W.-W. Yam, V. K.-M. Au, S. Y.-L. Leung, *Chem. Rev.* **2015**, *115*, 7589–7728.
[18] V. W.-W. Yam, K. K.-W. Lo, *Chem. Soc. Rev.* **1999**, *28*, 323–334.
[19] V. W.-W. Yam, K. M.-C. Wong, *Chem. Commun.* **2011**, *47*, 11579.
[20] G. Li, D. Zhu, X. Wang, Z. Su, M. R. Bryce, *Chem. Soc. Rev.* **2020**, *49*, 765–838.
[21] M. Dahlen, T. P. Seifert, S. Lebedkin, M. T. Gamer, M. M. Kappes, P. W. Roesky, *Chem. Commun.* **2021**, *57*, 13146–13149.
[22] M. Dahlen, E. H. Hollesen, M. Kehry, M. T. Gamer, S. Lebedkin, D. Schooss, M. M. Kappes, W. Klopper, P. W. Roesky, *Angew. Chem.* **2021**, *133*, 23553–23560; *Angew. Chem. Int. Ed.* **2021**, *60*, 23365–23372.
[23] M. Dahlen, M. Kehry, S. Lebedkin, M. M. Kappes, W. Klopper, P. W. Roesky, *Dalton Trans.* **2021**, *50*, 13412–13420.
[24] A. V. Paderina, I. O. Koshevoy, E. V. Grachova, *Dalton Trans.* **2021**, *50*, 6003–6033.
[25] C. Fliedel, A. Ghisolfi, P. Braunstein, *Chem. Rev.* **2016**, *116*, 9237–9304.
[26] Z. Yang, Z. Mao, X. Zhang, D. Ou, Y. Mu, Y. Zhang, C. Zhao, S. Liu, Z. Chi, J. Xu, Y.-C. Wu, P.-Y. Lu, A. Lien, M. R. Bryce, *Angew. Chem. Int. Ed.* **2016**, *55*, 2181–2185; *Angew. Chem.* **2016**, *128*, 2221–2225.
[27] J. Seixas de Melo, G. Quinteiro, J. Pina, S. Breda, R. Fausto, *J. Mol. Struct.* **2001**, *565–566*, 59–67.
[28] N. G. Bryantseva, I. V. Sokolova, R. M. Gadirov, V. P. Khilya, Y. L. Garazd, *J. Appl. Spectrosc.* **2009**, *76*, 813–818.
[29] Z. Feng, Y. Yu, X. Yang, D. Zhong, D. Song, H. Yang, X. Chen, G. Zhou, Z. Wu, *Inorg. Chem.* **2019**, *58*, 7393–7408.
[30] A. Jackel, M. Linseis, C. Häge, R. Winter, *Inorganics* **2015**, *3*, 55–81.
[31] H. Sun, H. Guo, W. Wu, X. Liu, J. Zhao, *Dalton Trans.* **2011**, *40*, 7834.
[32] W. Wu, S. Ji, W. Wu, J. Shao, H. Guo, T. D. James, J. Zhao, *Chem. Eur. J.* **2012**, *18*, 4953–4964.
[33] W. Wu, W. Wu, S. Ji, H. Guo, J. Zhao, *Dalton Trans.* **2011**, *40*, 5953.
[34] T. Yu, S. Yang, Y. Zhao, H. Zhang, D. Fan, X. Han, Z. Liu, *Inorg. Chim. Acta* **2011**, *379*, 171–174.
[35] G. Achar, P. Agarwal, K. N. Brinda, J. G. Małecki, R. S. Keri, S. Budagumpi, *J. Organomet. Chem.* **2018**, *854*, 64–75.
[36] G. Achar, S. C. R, S. A. Patil, J. G. Małecki, S. Budagumpi, *New J. Chem.* **2019**, *43*, 1216–1229.
[37] B. M. Geetha, J. G. Małecki, M. Alwarsamy, R. S. Keri, V. S. Betageri, S. Budagumpi, *J. Mol. Liq.* **2020**, *316*, 113809.
[38] Ł. Balewski, S. Szulta, A. Jalińska, A. Kornicka, *Front. Chem.* **2021**, *9*, 781779.
[39] J. Arcau, V. Andermark, E. Aguiló, A. Gandioso, A. Moro, M. Cetina, J. C. Lima, K. Rissanen, I. Ott, L. Rodríguez, *Dalton Trans.* **2014**, *43*, 4426–4436.
[40] C. Cunha, A. Pinto, A. Galvão, L. Rodríguez, J. S. Seixas de Melo, *Inorg. Chem.* **2022**, *61*, 6964–6976.
[41] V. Gallo, P. Mastrorilli, C. F. Nobile, P. Braunstein, U. Englert, *Dalton Trans.* **2006**, 2342–2349.
[42] F. Durap, N. Biricik, B. Gümgüm, S. Özkar, W. H. Ang, Z. Fei, R. Scopelliti, *Polyhedron* **2008**, *27*, 196–202.
[43] N. V. S. Harisomayajula, S. Makovetskyi, Y. C. Tsai, *Chem. Eur. J.* **2019**, *25*, 8936–8954.
[44] H. L. Hermann, G. Boche, P. Schwerdtfeger, *Chem. Eur. J.* **2001**, *7*, 5333–5342.
[45] R. Ahuja, M. Nethaji, A. G. Samuelson, *Polyhedron* **2007**, *26*, 142–148.
[46] N. Kathewad, S. Pal, R. L. Kumawat, M. Ehesan Ali, S. Khan, *Eur. J. Inorg. Chem.* **2018**, *2018*, 2518–2523.
[47] A. Ghisolfi, C. Fliedel, P. De Frémont, P. Braunstein, *Dalton Trans.* **2017**, *46*, 5571–5586.
[48] E. L. Muetterties, C. W. Alegranti, *J. Am. Chem. Soc.* **1970**, *92*, 4114–4115.
[49] H. Schmidbaur, A. Schier, *Angew. Chem. Int. Ed.* **2015**, *54*, 746–784; *Angew. Chem.* **2015**, *127*, 756–797.
[50] M. Baba, *J. Phys. Chem. A* **2011**, *115*, 9514–9519.
[51] G. Baryshnikov, B. Minaev, H. Ågren, *Chem. Rev.* **2017**, *117*, 6500–6537.
[52] H. Ma, Q. Peng, Z. An, W. Huang, Z. Shuai, *J. Am. Chem. Soc.* **2019**, *141*, 1010–1015.
[53] A. D. Nidhankar, Goudappagouda, V. C. Wakchaure, S. S. Babu, *Chem. Sci.* **2021**, *12*, 4216–4236.
[54] H. Uoyama, K. Goushi, K. Shizu, H. Nomura, C. Adachi, *Nature* **2012**, *492*, 234–238.
[55] S. Xu, Q. Yang, Y. Wan, R. Chen, S. Wang, Y. Si, B. Yang, D. Liu, C. Zheng, W. Huang, *J. Mater. Chem. C* **2019**, *7*, 9523–9530.
[56] T. J. Penfold, E. Gindensperger, C. Daniel, C. M. Marian, *Chem. Rev.* **2018**, *118*, 6975–7025.

Manuscript received: February 15, 2023
Accepted manuscript online: March 17, 2023
Version of record online: ■■, ■■

RESEARCH ARTICLE

Improving the shining hour: Coumarin-functionalized aminodiphosphine and its copper and silver complexes of different nuclearities have been synthesized. The complexes exhibit unusual persistent phosphorescence with a lifetime as long as 1.5 s in solution at 77 K that is strongly dependent on phase and temperature.

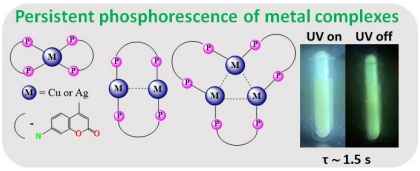

*V. R. Naina, Dr. A. K. Singh, P. Rauthe, Dr. S. Lebedkin, Dr. M. T. Gamer, Prof. Dr. M. M. Kappes, Prof. Dr. A.-N. Unterreiner, Prof. Dr. P. W. Roesky**